

Remote sensing of water quality in the Rotorua lakes

CBER Contract Report 51

Client report prepared for
Environment Bay of Plenty

by

Mathew G. Allan¹, Brendan J. Hicks¹, and Lars Brabyn²

mga1@waikato.ac.nz, b.hicks@waikato.ac.nz, larsb@waikato.ac.nz

¹Centre for Biodiversity and Ecology Research
Department of Biological Sciences
School of Science and Engineering
The University of Waikato
Private Bag 3105
Hamilton, New Zealand

²Department of Geography
Faculty of Arts and Social Sciences
The University of Waikato
Private Bag 3105
Hamilton, New Zealand

7 December 2007

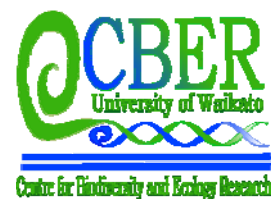


Table of Contents

	Page
Abstract.....	4
Introduction.....	5
Aims.....	7
Study site.....	7
Methods.....	8
Image pre-processing.....	8
Statistical analysis.....	9
Image sampling.....	9
Signature acquisition and regression models.....	10
Results and discussion	10
Conclusions.....	20
Future Work.....	21
Acknowledgements.....	21
References.....	22
Appendix 1. Water quality data from physical measurements (chl <i>a</i> concentration, Secchi depth, and turbidity; source: Environment Bay of Plenty, unpublished) and satellite data from Landsat 7 ETM+ images (B = band intensity).	26

List of tables

Table 1. Landsat 7 ETM+ band specifications (NASA specification table).....	5
Table 2. Landsat 7 ETM+ capabilities (NASA specification table).	5
Table 3. Summary of recent remote sensing studies of lake waters using Landsat imagery. (MSS – Multispectral Scanner, TM – thematic mapper, CHL – chlorophyll <i>a</i> , SEC – Secchi depth, TUR – turbidity, TSS – total suspended sediment, SPM – total suspended particulate material).	7
Table 4. Summary of Rotorua lakes physical characteristics including land cover as percentage of catchment area. Source: Scholes and Bloxham (2007).	8
Table 5. Environment Bay of Plenty Rotorua lakes sampling site locations (New Zealand Map Grid 1949). * Map location in format NZMS 260 map number: map reference.	10

List of figures

Figure 1. True colour composite image (standard deviation stretched) of the Rotorua lakes from 25 Jan 2002 of visible bands 1-3 from Landsat 7 ETM+.....	9
Figure 2. Rotorua lakes regression of chlorophyll <i>a</i> concentration in $\mu\text{g/L}$ against Band 1/Band 3 from ground data and a Landsat 7 ETM+ image from 25 Jan 2002.....	11
Figure 3. Raw residuals vs. predicted values from regression in Fig. 2 (equation 1).....	12
Figure 4. Rotorua lakes regression of chl <i>a</i> concentration in $\mu\text{g/L}$ against Band 1/Band 3 from ground data and a Landsat 7 ETM+ image from 24 Oct 2002.....	12
Figure 5. Raw residuals vs. predicted values from regression in Fig. 4 (equation 2).....	13
Figure 6. Overlaid regressions for chl <i>a</i> concentration from ground data against Band 1/Band 3 from 25 Jan 2002 and 24 Oct 2002 Landsat images (see Figures 2 and 4).....	15
Figure 7. Regression of Secchi depth in m against Band 1/Band 3 of a Landsat 7 ETM+ image from 25 Jan 2002 in the Rotorua lakes.....	15
Figure 8. Regression between average 2002 Trophic Lake Index (calculated from measured values of chl <i>a</i> , Secchi depth, and N and P concentration, Gibbons_Davies, 2003) against Band 1/Band 3 from a Landsat 7 ETM+ image from 25 Jan 2002).	16
Figure 9. Chl <i>a</i> concentrations in $\mu\text{g/L}$ in the Rotorua lakes and Lake Taupo on 25 Jan 2002 predicted from equation 1.....	17
Figure 10. Chl <i>a</i> concentrations in $\mu\text{g/L}$ in the Rotorua lakes and Lake Taupo on 24 Oct 2002 predicted from equation 2.....	18
Figure 11. Chl <i>a</i> concentrations in $\mu\text{g/L}$ in the Rotorua lakes on 24 Oct 2002 predicted from equation 2.	19
Figure 12. Chl <i>a</i> concentrations in $\mu\text{g/L}$ in the Rotorua lakes on 6 Jan 2001 predicted from equation 1.	19
Figure 13. Chl <i>a</i> concentrations in $\mu\text{g/L}$ in lakes Rotoehu (left) and Rotoiti (right) on 6 Jan 2001 predicted from equation 1.....	20

Reviewed by:



Kevin J. Collier

Approved for release by:



David P. Hamilton

Abstract

The aim of this study was to determine empirical models between Landsat imagery and lake water quality variables (chlorophyll (chl) *a* and Secchi depth) to enable water quality variables to be synoptically quantified. These models were then applied to past satellite images to determine temporal patterns in the spatial variation of water quality. Monitoring of lakes using traditional methods is expensive and lacks the ability to effectively monitor the spatial variability of water quality within and between lakes. Remote sensing can provide truly synoptic assessments of water quality, in particular the spatial distribution of phytoplankton. Recent studies monitoring lake water quality using Landsat series platforms have been successful in predicting water quality with a high accuracy. Analysis was carried out on two Landsat 7 Enhanced Thematic Mapper (ETM+) satellite images of the Rotorua lakes and Lake Taupo, for which most *in situ* observations were taken within two days of image capture. Regression equations were developed between the Band 1/Band 3 ratios (B1/B3) from Landsat images from summer (25 Jan 2002) and spring (24 Oct 2002) and water quality variables measured in the lakes by Environment Bay of Plenty. For summer, the regression of *in situ* chl *a* concentration in µg/l from ground data against the Band 1/Band 3 ratio (B1/B3) was

$$\text{Ln chl } a = 14.141 - 5.0568 (\text{B1/B3})$$

($r^2 = 0.91$, $N = 16$, $P < 0.001$). For spring, the regression equation was

$$\text{Ln chl } a = 24.251 - 9.2806 (\text{B1/B3})$$

($r^2 = 0.83$, $N = 13$, $P < 0.001$). Chl *a* water quality maps were then produced using these models, which were also applied to other images without *in situ* observations near the time of image capture.

This technique proved useful for analysing spatial distribution of phytoplankton, especially in lakes Rotoiti and Rotoehu. The results from this investigation suggest that remote sensing of water quality provides meaningful and useful information with a range of applications and could provide information on temporal variability of water quality.

Introduction

The aim of remote sensing of lakes is to provide truly synoptic monitoring of water quality. Traditional point sampling using chemical and meter methods can be expensive and not effectively monitor the heterogeneity of water quality variables. Landsat Multispectral Scanner (MSS) imagery is available from 1972-1981, Landsat 5 Thematic Mapper (TM) was launched in 1984 and is still operating, and Landsat 7 Enhanced Thematic Mapper + (ETM+) was launched in 1999. The repeat cycle is 16 days, and each scene is 185 km wide and 120 km high (Table 1).

Table 1. Landsat 7 ETM+ band specifications (NASA specification table).

Band number	Spectral range (μm)	Ground resolution (m)
B1	0.450 to 0.515	30
B2	0.525 to 0.605	30
B3	0.630 to 0.690	30
B4	0.750 to 0.900	30
B5	1.55 to 1.75	30
B6	10.4 to 12.5	60
B7	2.09 to 2.35	30
Panchromatic	0.520 to 0.900	15

Landsat satellites record digital images of lakes and their catchments by recording electromagnetic radiation at distinct wavelengths or bands. The highest correlation between water quality variables and satellite signatures is found in the visible (0.4-0.7 μm) and near infrared (0.7-1.5 μm) spectrum which corresponds to Landsat bands 1- 4 (Curran 1985). The main factors that affect water clarity are phytoplankton, organic detritus, suspended sediment, and dissolved organic matter (DOM). These factors subsequently affect the water subsurface radiance reflectance measured by satellites (Bukata *et al.*, 1995).

Table 2. Landsat 7 ETM+ capabilities (NASA specification table).

Attribute	Value
Swath width:	185 km
Repeat coverage interval:	16 days (233 orbits)
Altitude:	705 km
Quantization:	Best 8 of 9 bits
On-board data storage:	~375 Gb (solid state)
Inclination:	Sun-synchronous, 98.2 degrees
Equatorial crossing:	Descending node; 10:00am +/- 15 min.
Launch vehicle:	Delta II
Launch date:	April 1999

Chlorophyll *a* (chl *a*) acts primarily as a differential absorber, causing a decrease in the spectral response at the blue end (450-520 nm) of the visible spectrum. Suspended solids are associated with increases in reflected energy at longer red wavelengths (630-690 nm) (Bukata *et al.*, 1995).

The dominant factors that affect water clarity in the Rotorua lakes are algal biomass and suspended sediment (Vant and Davies-Colley, 1986). Algal biomass was the dominant influence on water clarity in Lake Okaro (accounting for 68% of the variability), whereas Lake Rotorua water clarity was more often dominated by suspended sediment, although chl *a* was occasionally predominant.

Reliable estimates of lake water quality from remote sensing can be achieved without employing *in situ*, data but accuracy of estimates can be improved by using reference data for a limited number of lakes (Pulliainen *et al.*, 2001). Accurate estimates of spatial variation in water quality in Rotorua lakes may be possible using only a few *in situ* samples to calibrate models.

The Rotorua lakes are of recent volcanic origin (140,000 years old) and were mostly formed by explosion craters or as the result of subsidence associated with volcanic activity (Lowe and Green 1986). There are 12 main lakes in the Rotorua area that represent a wide range of lake geomorphology and water quality, which means this area is suitable for remote sensing as regression models cover a wide range of water quality (Olmanson *et al.*, 2001).

The Rotorua lakes fit into four categories based on their mixing regimes and trophic status. These are eutrophic monomictic (Okaro and Rotoiti), mesotrophic monomictic (Okareka, Tikitapu, Rotokakahi and Okataina), oligotrophic monomictic (Tarawera, Rotoma, and Rotomahana) and meso- and eutrophic polymictic lakes (Rotorua, Rotoehu, and Rerewhakaaitu) (Hamilton 2003).

Numerous investigations have shown that strong empirical relationships can be developed between Landsat Multispectral Scanner (MSS) or Thematic Mapper (TM) imagery and *in situ* measurements of water quality (Table 3). One of the first studies of lakes with satellites used MSS images in a reconnaissance analysis of lake condition in Minnesota (Brown *et al.*, 1977). Later Landsat imagery was used to generate a reliable prediction for chl *a* concentration in the Minnesota lakes, USA (Lillesand *et al.*, 1983), and determine long term Secchi depth trends from 13 images captured from 1973 to 1998, for which limited historical data was available in many instances (Kloiber *et al.*, 2002b).

Areas of interest (AOIs) with depths of at least 3 m or twice the Secchi depth are required for open water signature acquisition. The AOI or sampling frame must contain at least 8 pixels in smaller lakes and up to 1000 pixels in larger lakes (Kloiber *et al.*, 2001a). Large AOIs can have higher correlation to reference data due to the smoothing of radiometric noise (Lillesand *et al.*, 1983).

Table 3. Summary of recent remote sensing studies of lake waters using Landsat imagery. (MSS – Multispectral Scanner, TM – thematic mapper, CHL – chlorophyll *a*, SEC – Secchi depth, TUR – turbidity, TSS – total suspended sediment, SPM – total suspended particulate material).

Location	Sensor	Variable	Technique	Reference
Minnesota	TM, MSS, IKONOS	SEC, CHL, TUR	B1/B3 ($r^2=0.85$), ($r^2=0.93$)	Lillesand et al. (1983), Kloiber et al. (2002)
Norfolk Broads	TM	SEC, TSS, CHL	TM3, TM3/TM1 ($r^2=0.85$)	Baban (1993)
Lake Erken	TM	SPM, CHL	Chromaticity (Green: $r^2=0.93$)	Oestlund et al. (2001)
Lake Garda	TM	CHL	TM1/TM2, TM1/TM3 ($r^2=0.72$)	Zilioli and Brivio (1996)
Frisian Lakes	TM & Spot	CHL	Bio-optical modeling	Dekker et al. (2002)
Gulf of Finland	TM	CHL, TSS, SEC, TUR	Empirical Neural Network	Zhang et al. (2002)
Lake Balaton	TM	CHL	Mixture Modeling ($r^2=0.95$)	Tyler et al. (2006)
Lake Kinneret	TM	CHL	(TM1-TM2)/TM3	Mayo et al. (1995)

Aims

The aims of our study were to:

- 1) Formulate empirical models to predict water quality in all lake pixels using Landsat ETM+ satellite imagery combined with ground data.
- 2) Apply empirical models to another image for which ground data (within 2 days) was unavailable.
- 3) Visualise the spatial distribution of water quality within lakes.

Study site

We analysed images that showed the 12 main Rotorua lakes (Table 4, Fig. 1). Phosphorus is most often the limiting nutrient to algal growth in freshwater systems, but in the Rotorua lakes, nitrogen has also been shown to be a limiting nutrient (White *et al.*, 1985). More recent studies, however, suggest that with the predominance of internally regenerated nutrients in Lake Rotorua, phosphorus may be the limiting nutrient (Burger *et al.*, 2007). Water quality in lakes Rotorua, Rotoiti, Rotoehu, Okareka, and Okaro is either degraded or showing early signs of deterioration due to increased nutrient input resulting from the intensification of land use over recent decades. Much of the catchment has been converted to exotic forest, farmland and urban areas, which has lead to an increase in phosphorus and nitrogen loads. Management plans are either currently being developed or are in place and are focusing on reducing nutrient inputs through various methods. Internal loading of lakes due to past nutrient inputs and water quality deterioration can take decades to recover. A further problem in addressing eutrophication is that the time lags between nutrient inputs entering groundwater and subsequently entering lakes is considerable, as the mean residence times of water in different streams entering Lake Rotorua range from 15-130 years (Morgenstern and Gorden 2006).

Table 4. Summary of Rotorua lakes physical characteristics including land cover as percentage of catchment area. Source: Scholes and Bloxham (2007).

Lake name	Lake area (km ²)	Catchment area (km ²)	Depth (m)		Pasture (%)	Indigenous forest/scrub (%)	Exotic forest (%)
			Maximum	Mean			
Rotoiti	34.0	123.7	125.0	60.0	15.9	36.4	46.2
Rotorua	80.6	441.4	44.8	11.0	51.8	25.1	14.3
Rotoehu	8.0	49.2	13.5	8.2	34.2	33.4	32.0
Tarawera	41.3	143.1	87.5	50.0	19.7	62.4	16.0
Okataina	10.8	59.8	78.5	39.4	10.7	84.1	7.8
Rotoma	11.1	27.8	83.0	36.9	23.4	46.0	26.7
Rotomahana	9.0	83.3	125.0	60.0	43.2	39.7	16.3
Okareka	3.4	18.7	33.5	20.0	37.8	51.6	7.6
Rotokakahi	4.4	19.7	32.0	17.5	26.3	16.6	57.1
Tikitapu	1.5	6.2	6.2	18.0	7.0	74.3	17.9
Okaro	0.3	3.9	18.0	12.1	90.6	2.1	6.3
Rerewhakaaitu	5.3	37.0	15.8	7.0	75.3	7.2	15.2

Methods

We used ERDAS Imagine for image processing, following the methods of Kloiber *et al.*, (2002a). ArcInfo was used for the production of water quality maps and Statistica/Excel for statistical analysis. Physiochemical data (Secchi depth, chl *a*, TP, TN, and turbidity) for the Rotorua lakes was obtained from EBOP unpublished data (Appendix 1A and 1B). Physiochemical data for Lake Taupo was taken from Gibbs (2004). Sixteen sampling stations (AOIs corresponding to EBOP and Environment Waikato sampling locations) were used in the 25 Jan 2002 regression (including two from Taupo). Thirteen sampling stations (including three from Taupo) were used for the 24 Oct 2002 regression.

Image pre-processing

We examined two images covering a 185 km by 185 km area, taken on 25 Jan 2002 and 24 Oct 2002. The Jan 2002 image (NASA Landsat Program, 2002, Landsat ETM+ scene path 72, row 86, USGS, Sioux Falls, 24 January 2002) was pre-processed by Landcare Research New Zealand (resampled to 15 m pixel size, NZMG) for MAF (Ministry of Forest and Agriculture) and subsequently obtained by The University of Waikato Department of Geography. The October 2002 image (NASA Landsat Program, 2002, Landsat ETM+ path 72, row 87, USGS, Sioux Falls, 23 October 2002, Universal Transverse Mercator projection) was acquired free of charge though the GLCF (Global Land Cover Facility) website.

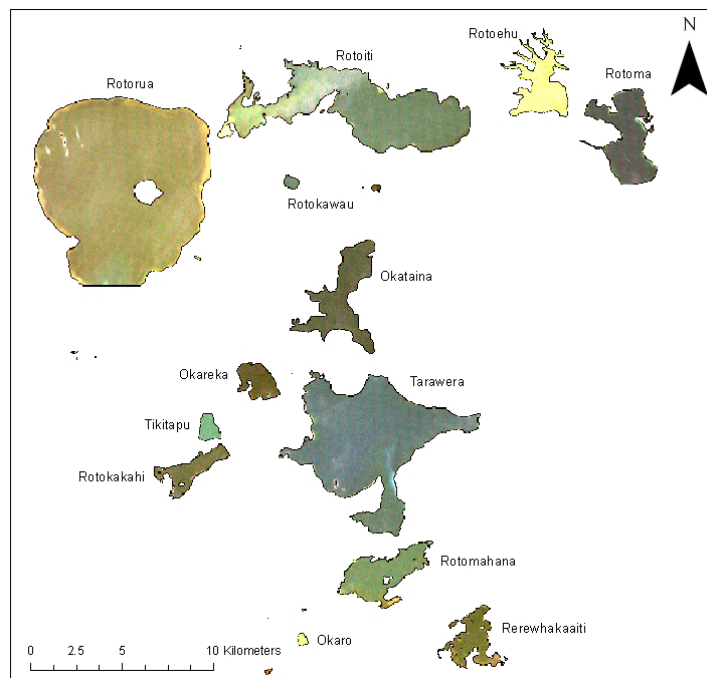


Figure 1. True colour composite image (standard deviation stretched) of the Rotorua lakes from 25 Jan 2002 of visible bands 1-3 from Landsat 7 ETM+.

Statistical analysis

Image sampling

A water-only image was initially created to confine data analysis areas to the lake water surface and to create a base for pixel level classification maps of water quality parameters. Image pixels were initially grouped into ten classes using the isocluster algorithm in ERDAS Imagine, which produced a new thematic coverage. This classification identified statistical patterns in the data and classified the data into ten classes based in the spectral response in bands 1-7 (excluding the thermal band 6), creating a new coverage or map that was then used as a binary mask to remove terrestrial areas from the image.

Unsupervised classification of the water-only image using 10 classes was then undertaken to highlight areas affected by reflectance from aquatic vegetation, shoreline and bottom sediment. These pixels were easily identified as they had elevated brightness in the near infra-red.

The sampling depth of remote sensing instruments depends on the attenuation of light in water. Electromagnetic radiation in the visible spectrum penetrates further in water with low phytoplankton, suspended sediment, and DOM. This means that in shallow waters, part of the reflectance signature may be composed of bottom reflectance.

Signature acquisition and regression models

The mean brightness for each AOI location (Table 5) was exported to Excel for regression model formulation (10 by 10 cell AOI). A Pearson correlation matrix between *in situ* water quality variables, and average band brightness values and various band ratios was used to indicate which bands are most suitable for creating regression models. Residual analysis was undertaken for all regression models to check that residuals are independent, and normally distributed. Pixel-level water quality maps were then produced for chl *a* by applying the formulated regression models to each pixel.

Table 5. Environment Bay of Plenty Rotorua lakes sampling site locations (New Zealand Map Grid 1949). * Map location in format NZMS 260 map number: map reference.

Lake name	Site	EBOP		NZMG	NZMG
		Reference	Map location*	Easting	Northing
Rotoma	65 m basin	BOP130007	V15:2495-4336	2824950	6343360
Okataina	65 m basin	BOP130009	V16:1060-3750	2810600	6337500
Rotoiti	Site 3	BOP130005	U15:0494-4619	2804940	6346190
Rotoiti	Site 4	BOP130059	V15:1078-4503	2810780	6345030
Rotoiti	Okawa Bay (mid bay)	BOP130047	U15:0278-4506	2802780	6345060
Rotoehu	Central main basin	BOP130029	V15:2044-4706	2820440	6347060
Rotorua	Site 2	BOP130002	U16:9800-3950	2798000	6339500
Rotorua	Site 5	BOP130027	U15:9820-4320	2798200	6343200
Tarawera	Site 5 (80 m depth)	BOP130030	V16:1000-2800	2810000	6328000
Okareka	Site 1 (32 m masin)	BOP130013	U16:0440-3180	2804400	6331800
Tikitapu	25 m basin	BOP130012	U16:0180-2880	2801800	6328800
Rotomahana	Site 2	BOP130060	V16:1108-2084	2811080	6320840
Rerewhakaaitu	Main lake (13 m basin)	BOP130014	V16:1629-1798	2816290	6317980
Okaro	18 m basin	BOP130017	U16:0690-1710	2806900	6317100

Results and discussion

There were strong relationships between chl *a* measured in $\mu\text{g/L}$ and B1/B3 ratio for the summer (January) and spring (October) 2002 images. For the summer image (25 Jan 2002), the regression equation was

$$\text{Ln chl } a = 14.141 - 5.0568 (\text{B1/B3}) \quad \text{equation 1,}$$

for which $r^2 = 0.91$, $N = 16$, and $P < 0.001$ (Fig. 2). Lake Tarawera showed the highest B1/B3 ratio (Fig. 2), indicating that it had the lowest chl *a*, although Lake Okareka was recorded as having the lowest *in situ* chl *a*. Lake Rotoiti has the lowest B1/B3 ratio and highest *in situ* chl *a*. Rotoehu has the largest residual (Fig. 3) in the January image and it is probably an outlier. This may be caused by the uncertainty of using one point sample to measure the highly heterogeneous chl *a*. The intense algal bloom observed near the sampling station may mean that chl *a* concentration could undergo rapid temporal fluctuations. Okawa Bay in Lake Rotoiti and Lake Okareka also had high residual values (Fig. 3).

For the spring image (24 October 2002), the regression equation was

$$\text{Ln chl } a = 24.251 - 9.2806 (\text{B1/B3}) \quad \text{equation 2,}$$

for which $r^2 = 0.83$, $N = 13$, and $P < 0.001$ (Fig. 4). Lake Okaro had the largest residual (Fig. 5). The *in situ* chl *a* was 89.1 $\mu\text{g/L}$ but the B1/B3 ratio is much lower than expected. A possible explanation for this was the time difference between the *in situ* chl *a* sampling (22 Oct 2002) and the image capture (24 Oct 2002). Algal blooms often consist of rapid rises in cell numbers followed by a collapse as nutrients and light become limiting. In addition, buoyancy variations, compounded with diurnal stratification, can cause rapid changes in chl *a* concentrations (e.g., Oliver and Ganf 2000). In Lake Rotorua, for instance, many blooms are transient and are not followed by a collapse necessarily. Often they are simply an interaction of large cyanobacterial biomass combined with diurnal stratification of the surface mixed layer, allowing the positively buoyant cells to congregate at the water surface; this is often disrupted on a daily basis, e.g., by an afternoon wind. These time scales mean that timing of image collection should be carefully recorded and assessed with regard to potential for this surface aggregation process (D. P. Hamilton, pers. comm.). Alternatively, this large residual may be caused by errors associated with using a single monitoring station where chl *a* has a large spatial variation (Kallio *et al.*, 2003).

The slopes of the regressions from the Jan and Oct 2002 images were significantly different (Fig. 6, ANCOVA $P < 0.001$). The two relationships shared the same centroid but had different slopes and intercepts. The difference between the two relationships could have been caused by a number of factors including different processing and resampling levels in the two images, different species of phytoplankton, and atmospheric effects.

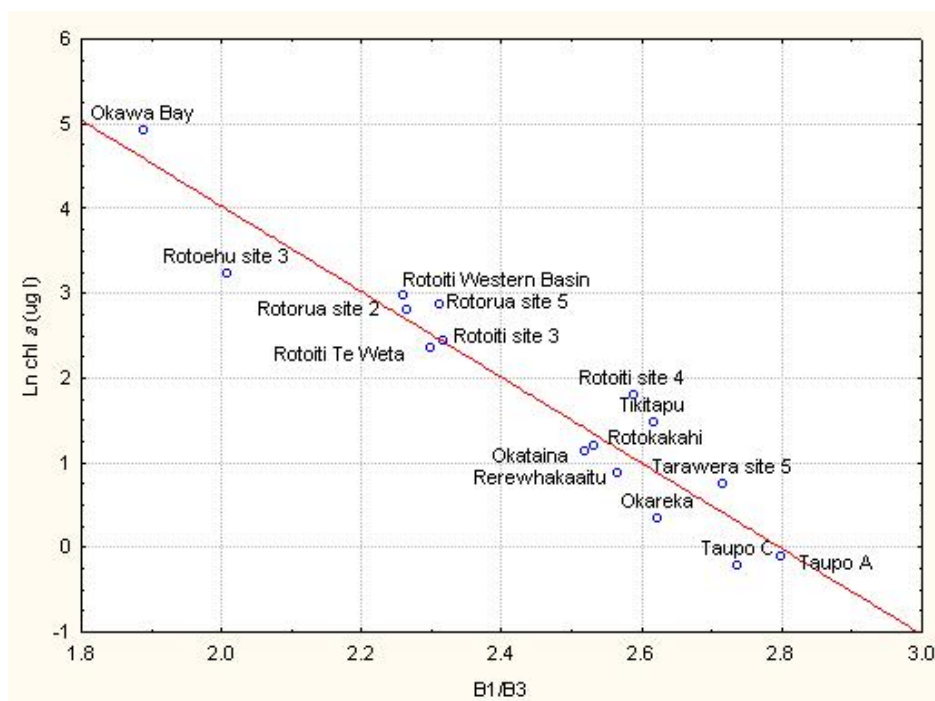


Figure 2. Rotorua lakes regression of chlorophyll *a* concentration in $\mu\text{g/L}$ against Band 1/Band 3 from ground data and a Landsat 7 ETM+ image from 25 Jan 2002.

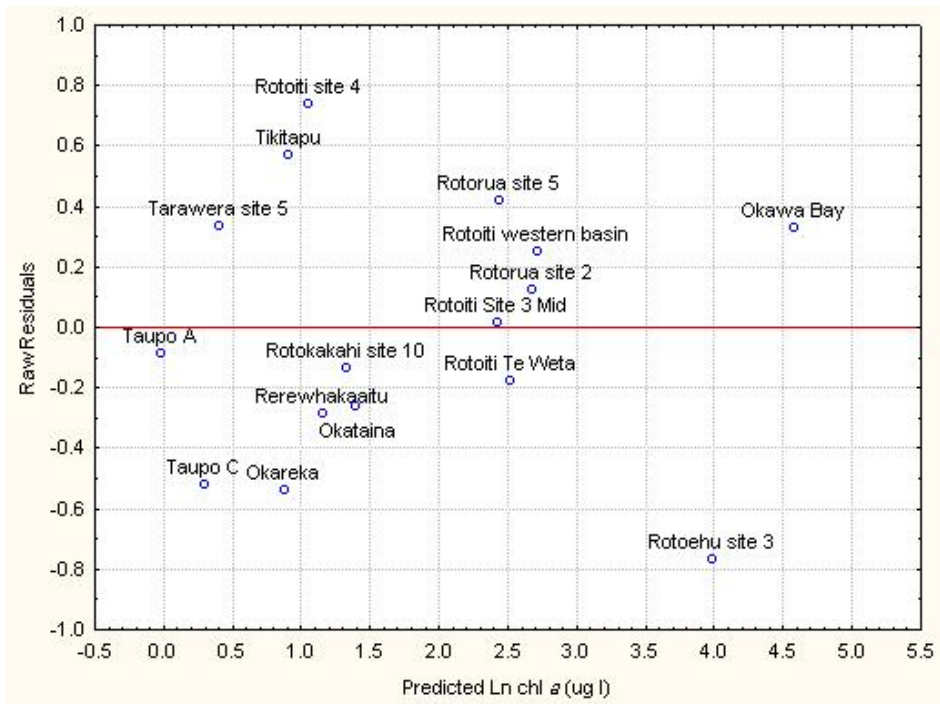


Figure 3. Raw residuals vs. predicted values from regression in Fig. 2 (equation 1).

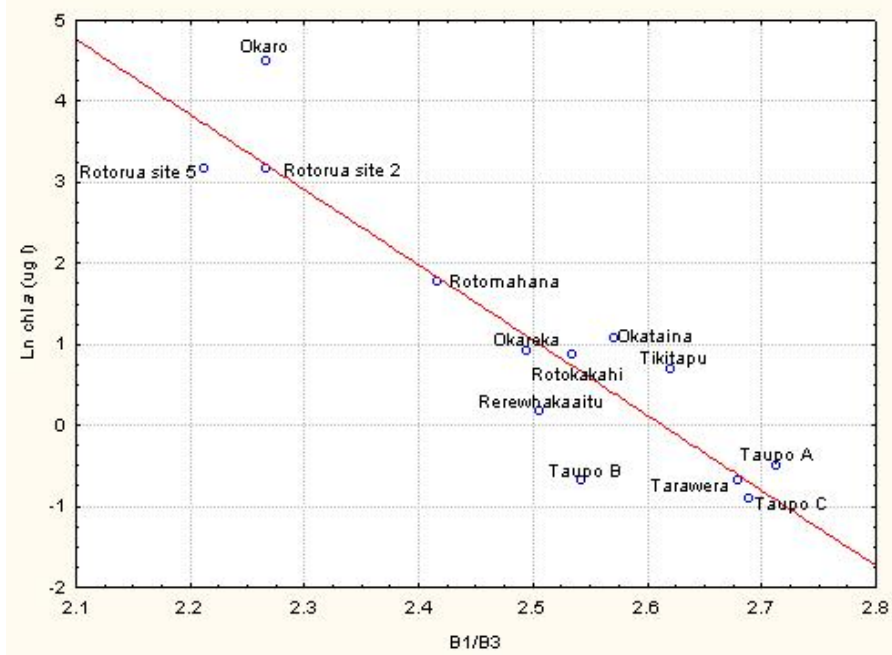


Figure 4. Rotorua lakes regression of chl *a* concentration in $\mu\text{g/L}$ against Band 1/Band 3 from ground data and a Landsat 7 ETM+ image from 24 Oct 2002.

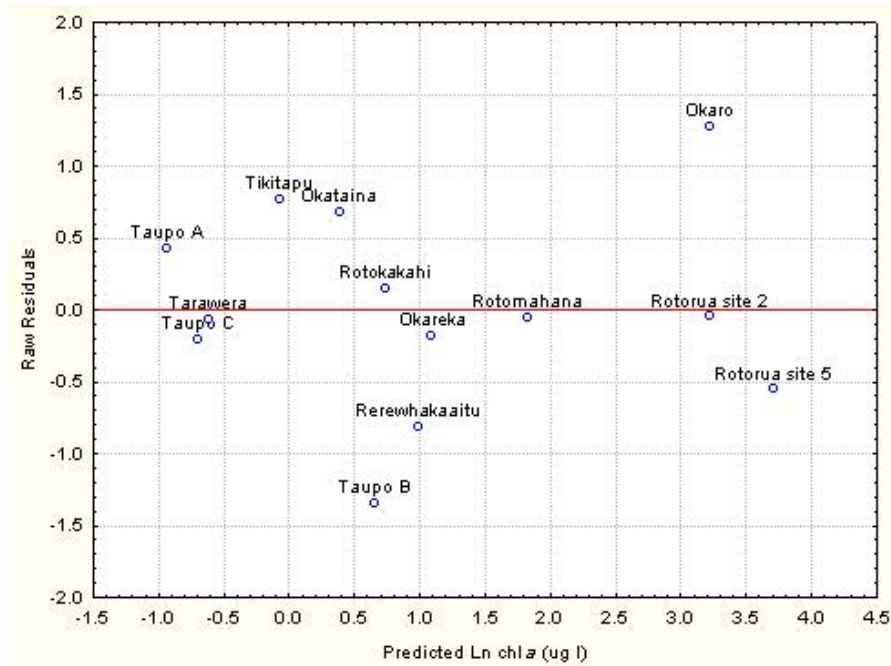


Figure 5. Raw residuals vs. predicted values from regression in Fig. 4 (equation 2).

Secchi depth (SD) in m showed a strong relationship with B1/B3 (Fig. 7). Okawa Bay in Lake Rotoiti (western end) had a Secchi depth of 0.78 m whereas in the eastern end SD was 4.29 m. The regression equation was

$$\text{Ln SD} = -5.2163 + 2.7753*(\text{B1/B3}) \quad \text{equation 3,}$$

for which $r^2 = 0.82$, $N = 14$, and $P < 0.001$. 2002 average Trophic Lake Index (TLI) taken from Gibbons-Davies (2003) also showed a strong relationship to B1/B3 (Fig. 8), with the regression equation

$$\text{TLI} = 11.2467 - 3.0985*(\text{B1/B3}) \quad \text{equation 4,}$$

for which $r^2 = 0.83$, $N = 10$, and $P = 0.0002$. TLI is an index composed of chl *a*, Secchi depth, total phosphorus concentration (TP), and total nitrogen concentration (TN), so it is not surprising that a strong relationship exists as all of these factors have the potential to affect water colour and clarity and are interrelated (Burns *et al.*, 1999).

In February 2002, chl *a* ranged from 6 µg/L in the eastern end of Lake Rotoiti to 136 µg/L in Okawa Bay, corresponding to variation in water colour from blue to yellow/green (Fig. 9). This image was captured in late summer, when algal blooms were clearly visible in Okawa Bay, Lake Rotoehu, and Lake Okaro. In the 2002 image of Okawa Bay it seems that the bloom event is significantly affecting water quality in the western bay area of Lake Rotoiti. The main reasons for the increase in incidence of severe algal blooms in Okawa Bay are the shallow sheltered nature of the bay and possibly input of nutrients through the lake bed or from septic tank leakage. Quantitative information on water quality in Okawa Bay was not available before 1997 (Ray *et*

al., 2002). Remote sensing may be able to address this lack of data through retrospective analysis of past Landsat images.

Spatial variation in lakes with high productivity can be large, meaning traditional point sampling methods can misrepresent the general lake condition. Using a single monitoring station can over or underestimate chl *a* by 29 – 34% (Kallio *et al.*, 2003). The areas of higher concentration (red colour) provide possible insights into the hydrodynamics of Lake Rotoehu as this area corresponds to a change in bathymetry to deeper areas to the west. Strong NW winds (about 30 km/h) were recorded on the day of image capture which may be responsible for the higher concentration in the SE of Lake Rotoehu. In October, chl *a* was higher in the southern end of Lake Taupo as indicated by the lighter colour (Fig. 10). Lake Taupo often exhibits a winter surface chl *a* maximum. Lake Rotorua also showed relatively high chl *a* concentration (23 µg/L) for winter (Fig. 10). A close-up of Fig. 10 shows the chl *a* distribution in the Rotorua lakes (Fig. 11).

Using equation 1, we predicted chl *a* distribution in an earlier image from summer (5 Jan 2001; Figs 12 and 13). Lake Rotoehu and Okawa Bay, Lake Rotoiti, again show high chl *a* concentrations (Fig. 13). On the 6 Jan 2001 image, high concentrations of chl *a* occurred in the central west of Lake Rotoehu, in contrast to spatial variability in 2002 (Fig. 13). Light westerly winds (5.5 km/h) were recorded near the time of this image capture, but do not seem to have had a visible effect on the concentration patterns.

We also investigated a three-band model for the 25 Jan 2002 Landsat 7 ETM+ image. The regression between measured chl *a* concentration in µg/L and bands 1, 2, and 3 (B1, B2, B3) was

$$\text{Ln chl } a = -7.8004 \cdot (B1 - B3) / B2 + 9.0704 \quad \text{equation 5,}$$

for which $r^2 = 0.91$, $N = 16$, and $P < 0.001$. This three-band model had a slightly higher r^2 value than the two-band model (equation 1).

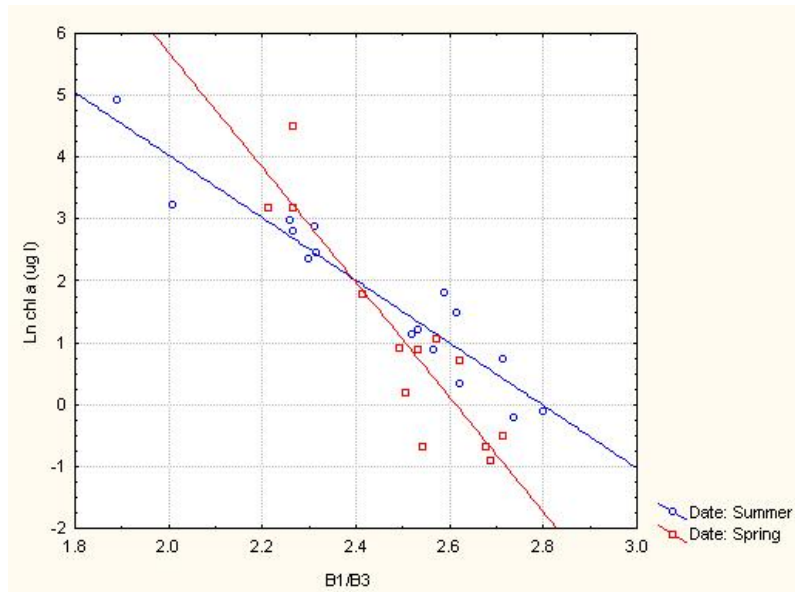


Figure 6. Overlaid regressions for chl *a* concentration from ground data against Band 1/Band 3 from 25 Jan 2002 and 24 Oct 2002 Landsat images (see Figures 2 and 4).

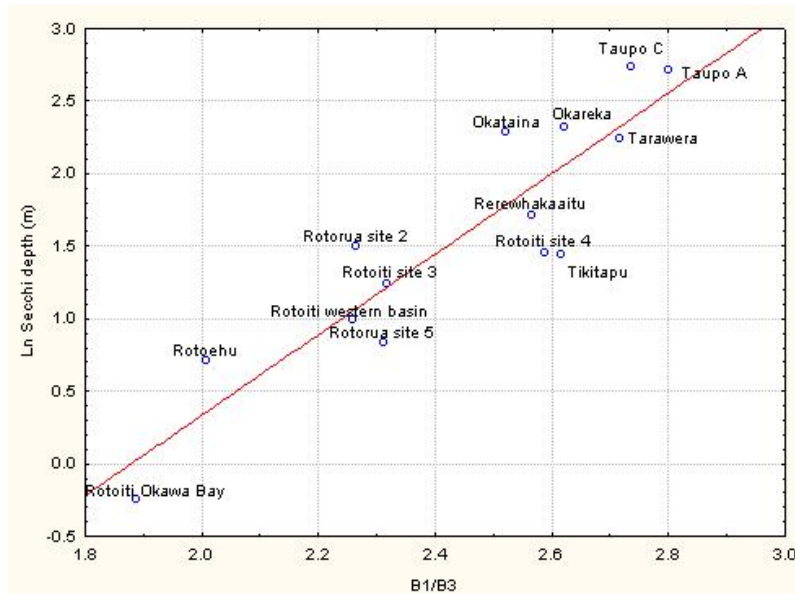


Figure 7. Regression of Secchi depth in m against Band 1/Band 3 of a Landsat 7 ETM+ image from 25 Jan 2002 in the Rotorua lakes.

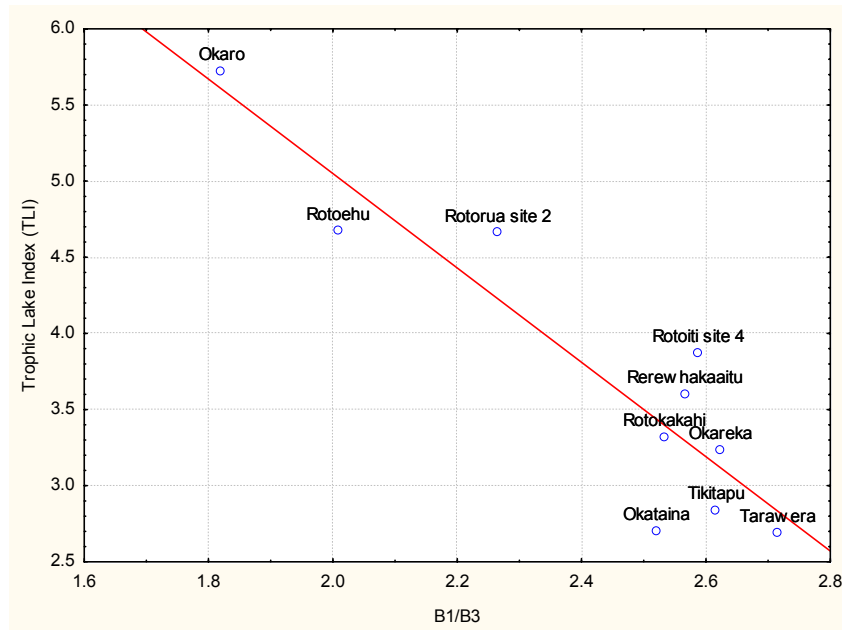


Figure 8. Regression between average 2002 Trophic Lake Index (calculated from measured values of chl *a*, Secchi depth, and N and P concentration, Gibbons-Davies, 2003) against Band 1/Band 3 from a Landsat 7 ETM+ image from 25 Jan 2002).

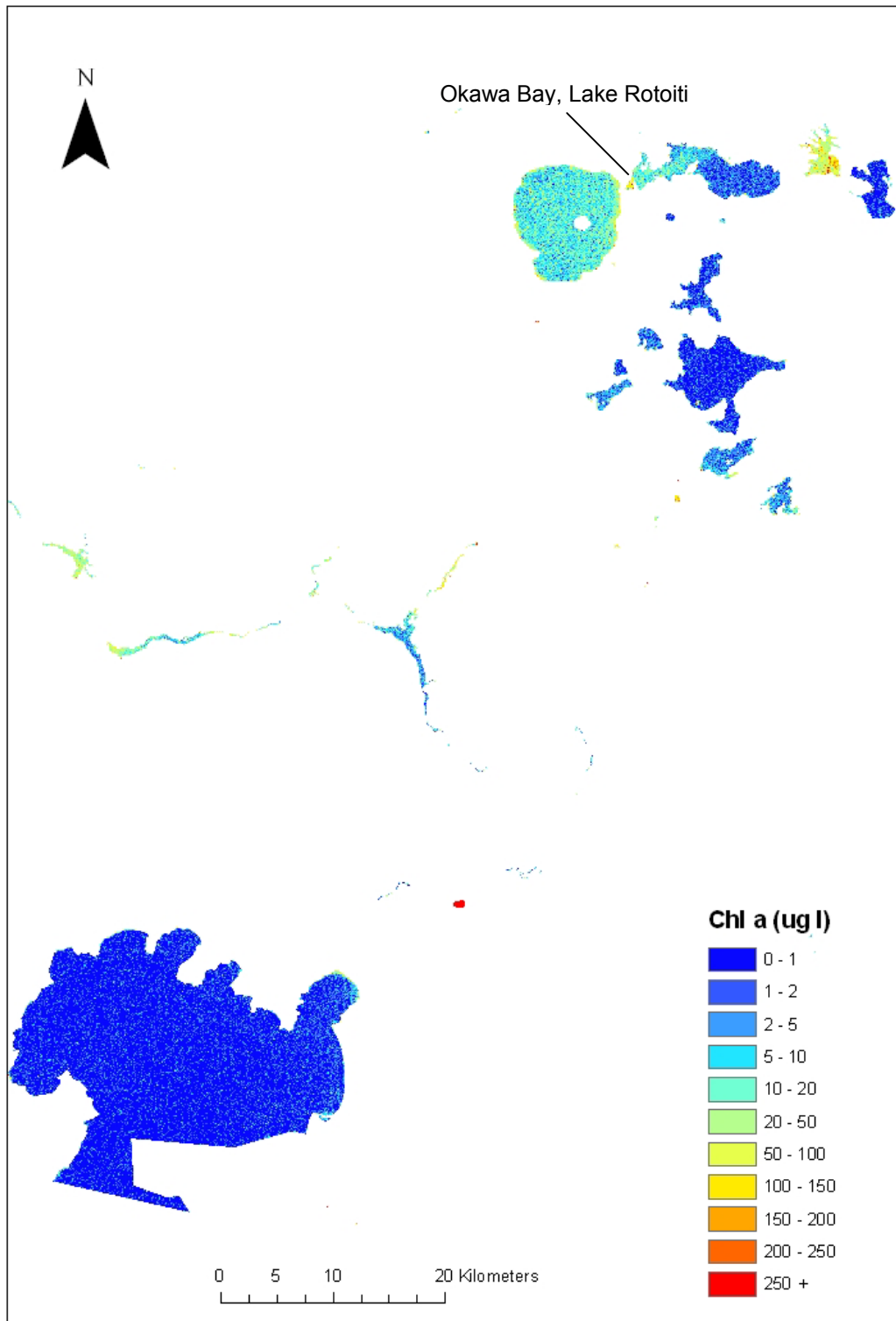


Figure 9. Chl *a* concentrations in $\mu\text{g/L}$ in the Rotorua lakes and Lake Taupo on 25 Jan 2002 predicted from equation 1.

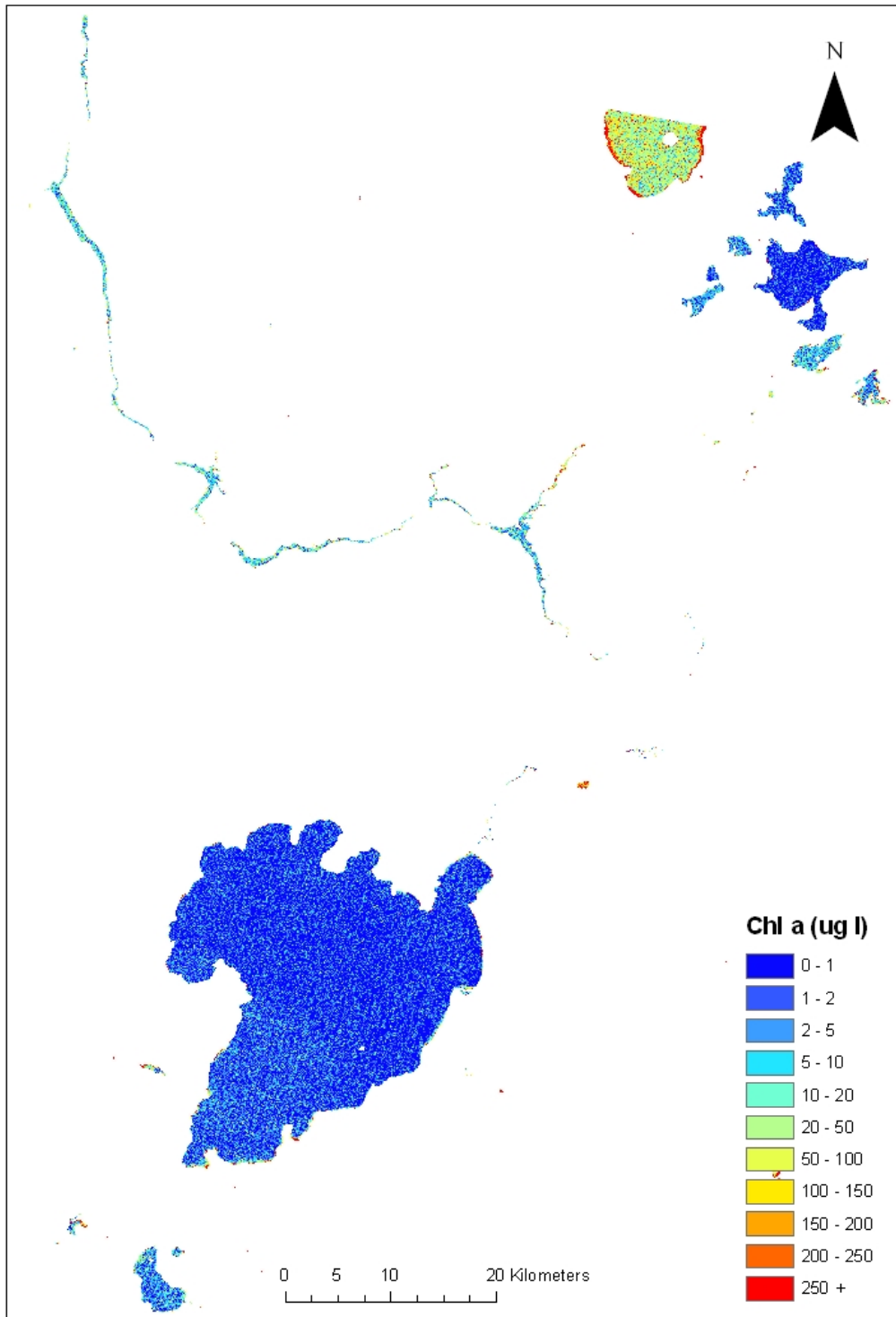


Figure 10. Chl *a* concentrations in µg/L in the Rotorua lakes and Lake Taupo on 24 Oct 2002 predicted from equation 2.

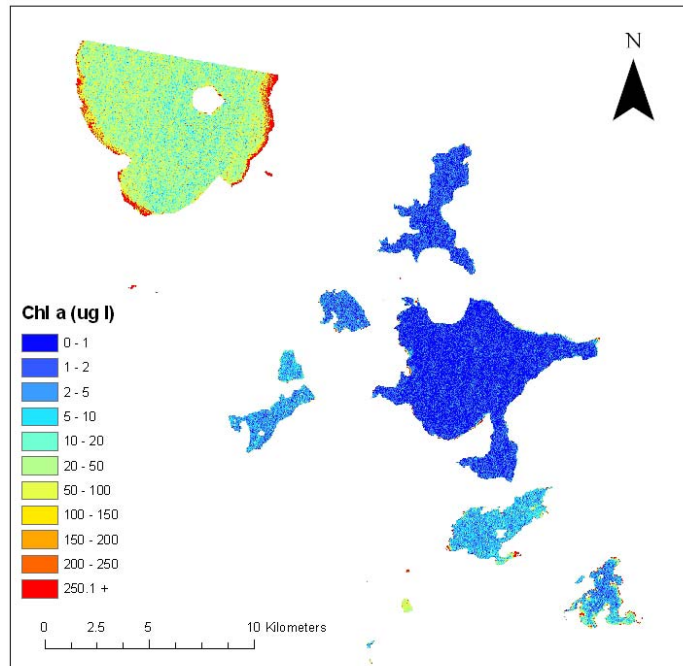


Figure 11. Chl *a* concentrations in $\mu\text{g/L}$ in the Rotorua lakes on 24 Oct 2002 predicted from equation 2.

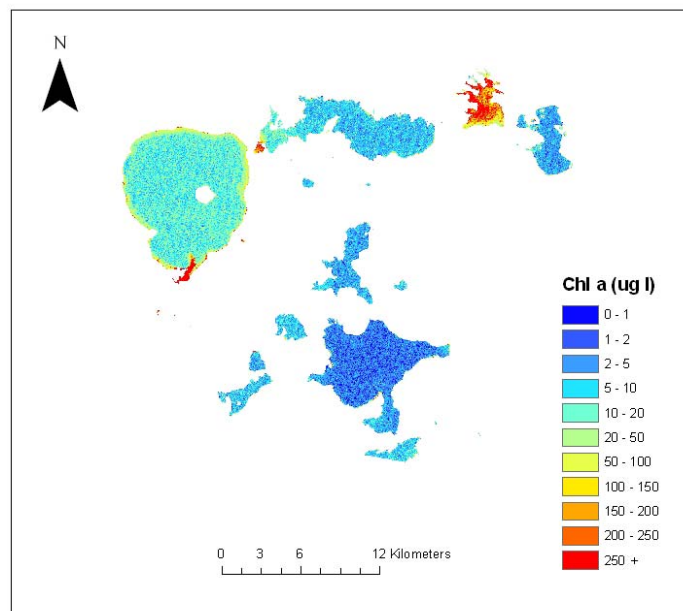


Figure 12. Chl *a* concentrations in $\mu\text{g/L}$ in the Rotorua lakes on 6 Jan 2001 predicted from equation 1.

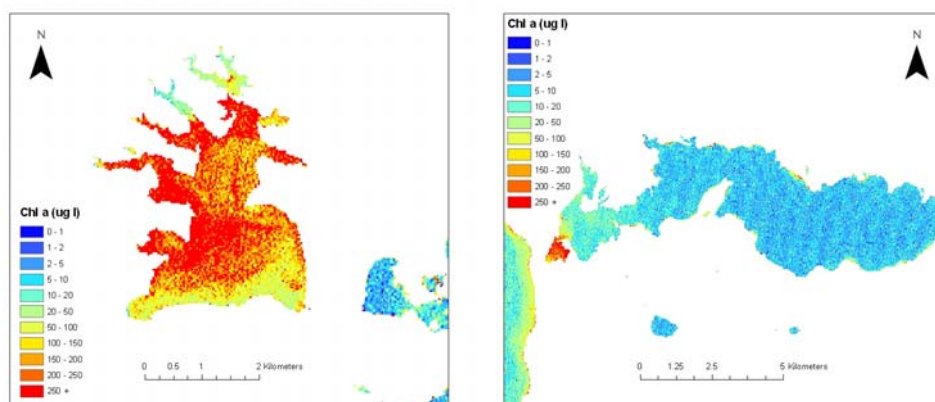


Figure 13. Chl *a* concentrations in µg/L in lakes Rotoehu (left) and Rotoiti (right) on 6 Jan 2001 predicted from equation 1.

Conclusions

Remote sensing provides synoptic predictions of water quality, which can aid our understanding of the patterns in spatial variation of water quality and its causes. When high within lake variation of chl *a* occurs, remote sensing can increase the accuracy of synoptic monitoring when combined with ground observations, by providing information on spatial variation.

The high correlation between B1/B3 and *in situ* chl *a* found in both Jan and Oct means that predictions spatial variability in water quality is possible when an image and ground data are present. Improvements in satellite data quality (processing level) and atmospheric correction could increase the temporal stability of the relationship meaning that it is possible to create a standard model which can be accurately applied to predict chl *a* concentration in images that do not have corresponding ground data.

High correlation between B1/B3 and Secchi depth means that pixel level water quality maps can also be created for this parameter. TLI also shows a strong relationship to B1/B3. TLI is based on the water quality parameters TN, TP, Secchi and chl *a* therefore it is not surprising that this relationship occurs. Pixel level maps of TLI may provide lake managers with a useful guide to pinpoint problem areas within individual lakes, such as Okawa Bay in Lake Rotoiti.

Chl *a* pixel-by-pixel concentration maps provide insight into spatial variability and can lead to an increase in the accuracy of monitoring in lakes with high spatial variation such as Rotoehu and Rotoiti. Monitoring of these lakes may need to include lake average chl *a* in the monitoring regime. In Jan 2002, intense algal blooms occurred and complex spatial variation in phytoplankton density can be seen in lakes Rotoiti and Rotoehu. The Jan 2001 image also showed large spatial variation in water quality in these lakes but with a different pattern occurring in Lake Rotoehu.

Limitations to monitoring water quality with Landsat data are the low temporal resolution which limits the utility in studies of dynamic processes. In addition, clear weather is needed on satellite overpass dates, which can mean some data is not suitable for use due to cloud cover. With the launch of numerous other satellites with comparable features to Landsat (such as ALOS and ASTER), the temporal resolution of image capture will be increased. Lakes characterised by high suspended sediment can often pose a problem as SSC can dominate spectral reflectance. Sub-pixel analysis may provide a solution to these problems.

Analysis of Landsat imagery has the advantage of having the longest continuous high resolution satellite data set, with the first Landsat MSS images taken in 1972. Temporal analysis of water quality trends could provide information on long term water quality trends, in spatial context. The Landsat Data Continuity Mission (LDCM) satellite is expected to launch in 2011 ensuring the continuation of this long running data set.

Future Work

If unprocessed images are purchased, digital numbers can be converted to at-satellite reflectance (which accounts for voltage bias and gain of the sensor, varying sun angle, and variation in Earth Sun distance). Subsequently, more confidence can be placed in atmospheric correction or image to image normalisation. A scene shift would be applied to these images which would encompass all of the Rotorua lakes and all of Lake Taupo in one image.

Also, two more recent Landsat 5 images from summer 2005 and spring 2006 exist with *in situ* Biofish data (taken within 2 days of image capture). Biofish provides a lateral 'snapshot' (depth and transect distance) of chl *a*, which would enable analysis of water quality in 3 dimensions. If all images are processed from raw data using standard reflectance conversion and atmospheric correction techniques a more direct comparison between images from Landsat 5 TM and Landsat 7 ETM+ will be possible.

Acknowledgements

This work was funded by the Foundation for Research, Science and Technology contract UOWX0505. We thank Environment Bay of Plenty for providing the measured data of water quality variables. Glenn Ellery, Paul Scholes, and Gareth Evans from Environment Bay of Plenty, also assisted. David Hamilton (University of Waikato) provided constructive advice on model development and the manuscript content. David Burger and Chris McBride helped with data collection. Salman Ashraf provided technical support. Kevin Collier (Environment Waikato) also provided valuable advice and comments.

References

- Baban MJ. 1993. Detecting water quality parameters in Norfolk Broads. *International Journal of Remote Sensing* 14: 1247-1267.
- Brown DR, Warwick R, Skaggs R. 1977. Reconnaissance analysis of lake condition in east-central Minnesota, p. 19 pp. Minnesota land management information system, Center for Urban and Regional Affairs, University of Minnesota, Minneapolis, MN, 19 pp.
- Bukata RP, Jerome JH, Kondratyev KY, Pozdnyakov DV. 1995. Optical properties and remote sensing of inland and coastal waters. CRC Press, Inc.
- Burger DF, Hamilton DP, Hall JA, Ryan EF. 2007. Phytoplankton nutrient limitation in a polymictic eutrophic lake: community versus species-specific responses. *Fundamental and Applied Limnology - Archiv für Hydrobiologie* 169: 57-68.
- Burns NM, Rutherford JC, Clayton JS. 1999. A monitoring and classification system for New Zealand lakes and reservoirs. *Lakes and Reservoir Management* 15: 255-271.
- Curran PJ. 1985. Principles of Remote Sensing. Longman Group (FE) Ltd.
- Dekker AG, Vos RJ, Peters SWM. 2002. Analytical algorithms for lake water TSM estimation for retrospective analysis of TM and SPOT sensor data. *International Journal of Remote Sensing* 23: 15-35.
- Gibbons-Davies, J. 2003. Rotorua Lakes Water Quality 2002. Environmental Publication 2003/02: ISSN 1175-9372. Environment Bay of Plenty, Whakatane, New Zealand.
- Hamilton DP 2003. An historical and contemporary review of water quality in the Rotorua lakes. Proceedings, Rotorua Lakes 2003, Practical Management for Good Lake Water Quality conference. pp. 3-15. [Keynote talk]

- Kallio K, Koponen S, Pulliainen J. 2003. Feasibility of airborne imaging spectrometry for lake monitoring-a case study of spatial chlorophyll *a* distribution in two meso-eutrophic lakes. *International Journal of Remote Sensing* 24: 3771-3790.
- Kloiber SM, Brezonik PL, Olmanson LG, Bauer ME. 2002a. A procedure for regional water clarity assesment using Landsat multispectral data. *Remote Sensing of Environment* 82: 38-47.
- Kloiber SM, Brezonik PL. 2002b. Application of Landsat imagery to regional-scale assessments of lake clarity. *Water Research* 36: 4330-4340.
- Lillesand TM, Johnson WL, Deuell RL, Lindstrom OM, Meisner DE. 1983. Use of Landsat data to predict the trophic state of Minnesota Lakes. *Photogrammetric Engineering and Remote Sensing* 49: 219-229.
- Lowe DJ, Green JD. 1987. Origins and development of lakes. Pages 1-64 *in* Viner, AB (ed). *Inland Waters of New Zealand*. DSIR Bulletin 241, Wellington.
- Mayo M, Gitelson A, Yacobi A, Ben-Avraham Z. 1995. Chlorophyll distribution in Lake Kinneret determined from Landsat Thematic Mapper data. *International Journal of Remote Sensing* 16: 175-182.
- Morgenstern U, Gordon D 2006. Prediction of future nitrogen loading to Lake Rotorua. GNS Science consultancy report 2006/10.
- Oestlund CP, Flink P, Stroembeck N, Pierson D, Lindell T. 2001. Mapping water quality in Lake Erken, Sweden, from Imaging Spectrometry and Landsat Thematic Mapper. *Science of the Total Environment* 268: 139-154.
- Oliver R, Ganf G. 2000. Freshwater blooms. Pages 149-194 *in* Whitton, B., and Potts, M. (eds), *The ecology of Cyanobacteria: their diversity in time and space*, The Netherlands: Kluwer Academic Publishers.

- Olmanson LG, Kloiber SM, Bauer ME, Brezonik PL. 2001. Image processing protocol for regional assessments of lake water quality. Water Resources Center and Remote Sensing Laboratory, University of Minnesota.
- Pulliainen, J, Kallio K, Eloheimo, K, Koponen S, Servomaa H, Hannonen T, Tauriainen S, Hallikainen M. 2001. A semi-operative approach to lake water quality retrieval from remote sensing data. *Science of the Total Environment* 268: 79-93.
- Ray D, Gibbs M, Broekhuizen N, Rutherford K, Stephens S. 2002. Okawa Bay water quality study. NIWA Client Report HAM2002-030. National Institute of Water and Atmospheric Research, Hamilton.
- Scholes, P. and M. Bloxham. 2007. Rotorua lakes water quality 2006 report. Environmental Publication 2007/12; ISSN 1175-9372. Environment Bay of Plenty, Whakatane, New Zealand.
- Gibbs, M. 2004. Lake Taupo Long-Term Monitoring Programme 2002-2003: Including Two Additional Sites. Environment Waikato Technical Report 2004/05; ISSN 1172-4005. Environment Waikato, Hamilton East, New Zealand.
- Tyler AN, Svab E, Preston T, Presing M, Kovacs WA. 2006. Remote sensing of the water quality of shallow lakes: A mixture modelling approach to quantifying phytoplankton in water characterized by high-suspended sediment. *International Journal of Remote Sensing* 27: 1521-1537.
- Vant WN, Davies-Colley RJ. 1986. Relative importance of clarity determinants in Lakes Okaro and Rotorua. *New Zealand Journal of Marine and Freshwater Research* 20: 355-363.
- White E, Law K, Payne S, Pickmore S. 1985. Nutrient demand and availability among planktonic communities – an attempt to assess nutrient limitation to plant growth in 12 Central Volcanic Plateau lakes. *New Zealand Journal of Marine and Freshwater Research* 19: 49-62.

Zhang Y, Pulliainen J, Koponen S, Hallikainen M. 2002. Application of an empirical neural network to surface water quality estimation in the Gulf of Finland using combined optical data and microwave data. *Remote Sensing of Environment* 81: 327-336.

Zilioli E, Brivio PA. 1996. The satellite derived optical information for the comparative assessment of lacustrine water quality. *The Science of the Total Environment* 196: 229-245.

Appendix 1. Water quality data from physical measurements (chl *a* concentration, Secchi depth, and turbidity; source: Environment Bay of Plenty, unpublished) and satellite data from Landsat 7 ETM+ images (B = band intensity).

A. Data associated with 25 Jan 2002 image.

Site	Date	Chl <i>a</i> (µg/L)	Secchi depth (m)	Turbidity (NTU)	B1	B2	B3	B1/B3	(B1-B3)/B2
Taupo site C	22-Jan-02	0.8	15.5		61.6	34.3	22.5	2.74	1.14
Taupo site A	22-Jan-02	0.9	15.0		61.9	34.7	22.1	2.80	1.15
Okareka site 1	23-Jan-02	1.4	10.2	0.57	57.9	33.9	22.1	2.62	1.06
Tarawera site 5	23-Jan-02	2.1	9.4	0.42	62.1	35.8	22.9	2.72	1.10
Rerewhakaaitu site 1	9-Jan-02	2.4	5.5	0.70	57.8	35.0	22.5	2.57	1.01
Okataina site 1	22-Jan-02	3.1	9.8	0.54	59.5	35.2	23.6	2.52	1.02
Rotokakahi site 10	23-Jan-02	3.3		0.69	59.3	35.2	23.4	2.53	1.02
Tikitapu site 1	23-Jan-02	4.4	4.2	0.85	62.2	39.9	23.8	2.62	0.96
Rotoiti site 4	22-Jan-02	6.0	4.3	0.95	61.2	37.3	23.6	2.59	1.01
Rotoiti Te Weta site	17-Jan-02	10.4		2.60	60.6	39.6	26.4	2.30	0.86
Rotoiti site 3	22-Jan-02	11.5	3.5	1.90	62.2	42.1	26.9	2.32	0.84
Rotorua site 2	23-Jan-02	16.5	4.5	2.20	59.6	38.2	26.3	2.27	0.87
Rotorua site 5	23-Jan-02	17.6	2.3	2.60	60.3	38.3	26.1	2.31	0.89
Rotoiti western basin site	24-Jan-02	19.4	2.7	3.30	62.6	42.9	27.7	2.26	0.81
Rotoehu site 3	22-Jan-02	25.0	2.0	2.60	62.8	49.0	31.3	2.01	0.64
Rotoiti Okawa Bay site	24-Jan-02	136.0	0.8	15.00	65.3	57.1	34.6	1.89	0.54

Appendix 1. (Continued).

B. Data associated with 24 Oct 2002 image.

Site	Date	Chl a ($\mu\text{g/L}$)	Secchi depth (m)	Turbidity (NTU)	B1	B2	B3	B1/B3	(B1-B3)/B2
Okareka site 1	24/10/2002	2.5	8.1	1.00	55.6	32.9	22.3	1.01	2.50
Okataina site 1	23/10/2002	2.9	7.5	0.67	56.0	31.8	21.8	1.08	2.57
Rotokakahi site 10	24/10/2002	2.4		0.68	57.1	34.5	22.5	1.00	2.53
Rotorua site 2	24/10/2002	23.8	1.9	3.50	58.4	38.1	25.8	0.86	2.27
Rotorua site 5	24/10/2002	23.6	1.9	4.60	58.1	38.3	26.3	0.83	2.21
Tikitapu site 1	24/10/2002	2.0	4.0	0.82	60.5	38.5	23.1	0.97	2.62
Okaro site 1	22/10/2002	89.1	1.3	4.50	56.5	39.4	24.9	0.80	2.27
Rerewhakaaitu site 1	22/10/2002	1.2	10.2		56.4	33.9	22.5	1.00	2.51
Rotomahana site 1	22/10/2002	5.9	2.9	1.30	57.1	35.4	23.6	0.95	2.42
Tarawera site 5	24/10/2002	0.5	8.4	1.40	59.8	34.4	22.3	1.09	2.68
Taupo site A	9/10/2002	0.6	15.5		58.2	32.2	21.4	1.14	2.71
Taupo site B	9/10/2002	0.5	15.0		58.3	33.1	22.9	1.07	2.54
Taupo site C	9/10/2002	0.4	19.0		58.6	32.4	21.8	1.13	2.69